Experimental Evaluation of AoA Estimation for UAV to Massive MIMO

Tarence Rice*, Divyanshu Pandey*, David Ramirez†, and Edward Knightly*

Department of Electrical Engineering, Rice University, Houston, TX *

DOCOMO Innovations Inc., Sunnyvale, CA†

{tmr7, dp76}@rice.edu, david.ramirez@docomoinnovations.com, knightly@rice.edu

Abstract—**This paper presents an evaluation of the performance of Angle of Arrival (AoA) estimation algorithms in Unmanned Aerial Vehicles (UAV) communication networks utilizing massive Multiple-Input Multiple-Output (MIMO) base stations. Five different AoA estimation algorithms were evaluated and their performance was assessed. The results show the impact of under-sampling on AoA estimation, specifically in the detection of multi-path with higher normalized power. The effects of azimuth AoA estimation via horizontal subarrays and the impact on multi-path AoA estimates for hovering drones were examined. The performance of the 2-D Bartlett spatial spectrum estimator was evaluated, demonstrating higher accuracy for both azimuth and elevation channels. This work provides important insights for system designers when designing massive MIMO to drone networks based on AoA estimation specifications.**

Index Terms—**Drone, Unmanned Aerial Vehicles, Angle of Arrival, Localization, Massive MIMO.**

I. INTRODUCTION

Unmanned Aerial Vehicles (UAVs) have various applications, including telecommunications and medical supply delivery [1]. Main aspects of deploying UAVs in telecommunication networks include three-dimensional deployment, performance analysis, channel modeling, and energy efficiency [2]. Using UAVs as relays can help overcome Non-Line-of-Sight (NLOS) propagation path challenges and enhance the likelihood of establishing Line-of-Sight (LOS) communication links, improving ground users' networks and providing cost-effective and easily deployable wireless transmission schemes [3].

The wireless environment poses challenges that can impact the accuracy of UAVs' Global Positioning System (GPS), cellular, and Wi-Fi localization, given its three dimensional mobility [4]. Massive Multiple-Input Multiple-Output (MIMO), with its ability to provide a large number of antennas for spatial processing, is an emerging technology that can significantly enhance network capacity and coverage for 5G and beyond 5G networks [5], [6]. It offers itself as a promising solution for UAV tracking. This paper analyzes the impact of flight and hovering mobility on the estimation of drone's Angle of Arrival (AoA) and how massive MIMO can improve the accuracy of such estimations, providing the first experimental evaluation of the interaction between UAVs and massive MIMO systems. By having the AoA for UAV applications

allows for more adaptive communication strategies and enhanced remote sensing capabilities.

In prior work [7], five classical AoA estimation algorithms were compared using MATLAB simulations on an eight-antenna uniform linear array (ULA). Our study experimentally evaluated these algorithms using an eight-antenna ULA and UAVs in real-world scenarios, providing insights into their practical limitations and advantages. Our findings showed Root-Multiple Signal Classification (R-MUSIC) performed best among the five algorithms for a hovering drone at various locations, while Bartlett provided additional environmental insights for angle estimation despite lower performance.

Fast-moving drones present challenges for accurate AoA estimation due to factors such as UAV mobility, wind, and fast time-varying multi-path. Our analysis of a hovering drone in a time-invariant channel revealed that accurate AoA estimation could be achieved with as few as 320 samples. This finding sheds light on the interplay between sampling rate, drone mobility, and the characteristics of the channel environment.

We studied the impact of antenna number and configurations on AoA estimation in massive MIMO systems. Furthermore, we analyzed the effect of using multiple rows and found that mobility and dynamic environments significantly impact AoA estimation accuracy. Additionally, we evaluated 2-D AoA estimation and found it to outperform multi-row/column methods, making it a practical application for joint azimuth and elevation estimation techniques in massive MIMO systems.

The remainder of this paper is organized as follows. Section II explains the theoretical methods employed in the study, while Section III provides details about the experimental platform. Section IV includes the experimental details, results and analysis. The paper is concluded in Section V.

II. SYSTEM MODEL AND METHODS

Multiple antennas are commonly used in AoA estimation to overcome challenges and improve accuracy. Factors such as antenna spacing, frequency, and the environment play crucial roles in determining the effectiveness of using multiple antennas. By carefully analyzing these factors, we can gain insights into optimizing AoA estimation techniques for improved performance.

We consider the system model from [7]. Assume a ULA with M antennas and equal antenna spacing of d. Let $x_m(n)$ denote the signal received by the mth antenna at the nth

sample index and $s_i(n)$ denote the input signal from the ith source, where $i = 1, \ldots, D$. The input output relation can be specified as:

$$x_m(n) = \sum_{i=1}^{D} s_i(n) e^{-j\beta d(m-1)\sin\theta_i} + w_m(n) \qquad (1)$$

where θ_i is the AoA of the ith signal, $\beta = 2\pi/\lambda$ where λ denotes the wavelength, and $w_m(n)$ denotes the additive noise term at the mth antenna. The signal source vector can be denoted as $\mathbf{s}(n) = [s_1(n), s_2(n), \ldots, s_D(n)]^T \in \mathbb{C}^{D \times 1}$ and the received vector as $\mathbf{x}(n) = [x_1(n), x_2(n), \ldots, x_M(n)]^T \in \mathbb{C}^{M \times 1}$. Subsequently, (1) can be written in vector form as:

$$\mathbf{x}(n) = \mathbf{A}(\boldsymbol{\theta})\mathbf{s}(n) + \mathbf{w}(n) \qquad (2)$$

where $\boldsymbol{\theta} = [\theta_1, \ldots, \theta_D]^T$ and $\mathbf{A}(\boldsymbol{\theta}) \in \mathbb{C}^{M \times D}$ is the array steering matrix defined as:

$$\mathbf{A}(\boldsymbol{\theta}) = \begin{bmatrix} 1 & 1 & \cdots & 1 \\ e^{-j\beta d \sin\theta_1} & e^{-j\beta d \sin\theta_2} & \vdots & e^{-j\beta d \sin\theta_D} \\ \vdots & \vdots & \ddots & \vdots \\ e^{-j\beta d(M-1)\sin\theta_1} & e^{-j\beta d(M-1)\sin\theta_2} & \cdots & e^{-j\beta d(M-1)\sin\theta_D} \end{bmatrix} \qquad (3)$$

and $\mathbf{w}(n) = [w_1(n), w_2(n), \ldots, w_M(n)]^T \in \mathbb{C}^{M \times 1}$ is the noise vector.

The objective of AoA estimation algorithms is to find the incident angles of arrival denoted by θ_i. For this, auto-correlation matrices of the received signals are required which are mostly not known in real-time measurements, and instead, are estimated from a finite number of data samples known as snapshots. Let K denote the number of snapshots, then an estimate of the auto-correlation matrix is computed as:

$$\hat{\mathbf{R}}_{\mathbf{xx}} = \frac{1}{K} \sum_{n=1}^{K} \mathbf{x}(n)\mathbf{x}^H(n) \qquad (4)$$

where $\mathbf{x}^H$ represents the Hermitian transpose of $\mathbf{x}$. Several algorithms exist to estimate $\boldsymbol{\theta}$ from the estimated auto-correlation. For instance, in Bartlett method, the output power or spatial spectrum as a function of θ_i is computed as:

$$P(\theta_i) = \mathbf{a}^H(\theta_i)\hat{\mathbf{R}}_{\mathbf{xx}}\mathbf{a}(\theta_i) \qquad (5)$$

where $\mathbf{a}(\theta_i)$ denotes the i-th column of the array steering matrix defined as:

$$\mathbf{a}(\theta_i) = [1, e^{-j\beta d \sin\theta_i}, \ldots, e^{-j\beta d(M-1)\sin\theta_i}]^T. \qquad (6)$$

By identifying the largest peaks of $P(\theta_i)$, we can accurately determine the AoA. A detailed theoretical description of several other approaches can be found in [8].

III. EXPERIMENTAL PLATFORM

This study integrates the Autonomous, Sensing, and Tetherless Networked Drones (ASTRO) platform [9] with the RENEW and Sounder software. The Reconfigurable Ecosystem for Next-Generation End-to-End Wireless (RENEW) testbed [10], developed at Rice University, is utilized, with the

Sounder framework enabling clients to send pilots and data to the base station and record received signals from all antennas. Transmit pilots are sent with Time Division Duplexing (TDD), and each client uses uplink signals on subframes, with a 3.6 GHz center frequency, a 5 MHz bandwidth and a sample rate of 5 MHz.

The TDD schedule is decomposed into frames, slots, pilots, and samples as shown in Fig. 1. A total of 2000 frames were collected during the experiment. Within each frame of 8.96 milli-seconds, there are 40 slots that include beacon, guard band, and pilot signals. Beacons synchronize clients, guard bands fill the buffer and provide spacing, and the pilots consist of long-term training sequences (LTS) of 1,120 samples. During the 17.92-second experiment, the base station collected 2,240,000 samples at each measurement location from signals transmitted by a single drone. These samples corresponded to the known pilot signals and were used to determine the AoA of the impinging signals at each site.
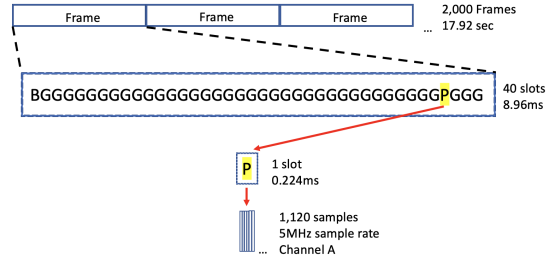

Fig. 1: Data sets as represented in frames, slots, and samples.

The base station was positioned at a height of 34 meters horizontal with the eight yard line. We measured at five positions, as shown in Fig. 2, at angles of $-9.64°$, $10.20°$, $21.54°$, $32.49°$, and $44.26°$, to evenly cover the Rice University football stadium. The drone hovered at each position for 17.92 seconds, providing a comprehensive view of the channel and allowing us to assess the impact of each location on AoA estimation performance.
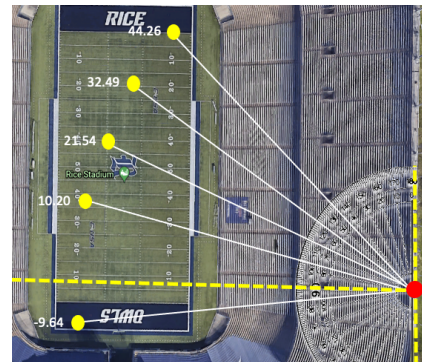

Fig. 2: Setup for AoA experiment at Rice football stadium.

The following experiments were conducted using the setup described above, detailed in Section IV:
- Evaluation of five different AoA estimation algorithms for fixed antenna configuration and number of samples.

- Analysis of the significance of sample count with fixed antenna configuration on AoA estimation.
- Investigation of the impact of different antenna configurations on AoA estimation accuracy for fixed sample count.
- Exploration of multi-row estimation with simultaneous averaging of multiple rows.
- Comparison of the performance of 2-D AoA estimation with multi-row and column estimation.

IV. Experimental Data and Results

A. AoA Estimation Algorithms

We analyze the accuracy of five classical AoA estimation algorithms for incoming signals from hovering drones. The algorithms include Bartlett, Minimum Variance Distortionless Response (MVDR), Multiple Signal Classification (MUSIC), R-MUSIC and Estimation of Signal Parameter via Rotational Invariance (ESPRIT) and their performance was assessed in terms of AoA estimation accuracy and robustness to environmental changes. This study provides valuable insights for selecting the most appropriate algorithm for drone applications.

Setup: We conducted an outdoor drone experiment at Rice Stadium, utilizing a transmitter client connected to a drone. This drone facilitated up-link traffic communication with a 32-antenna massive MIMO base station, where 16 or more antennas represent the massive aspect. The angles were defined as zero degrees when measured at the front of the base station. The drone's locations were mapped using GPS positioning and flown at a 20 m hovering altitude. To compare estimation algorithm performance, we collected data as described in Section III using only eight planar array elements with 3.94 cm spacing between them to gather a baseline for further experiments. All 2,240,000 samples collected were used to estimate the AoA at each location.

Results and Findings: Fig. 3 presents a comprehensive comparative analysis of five algorithms. This is depicted through the use of box plots which for each set of AoA methods displays the median, minimum score, lower quartile of 25%, upper quartile of 75%, maximum score, and outliers.

Fig. 3a shows that the Bartlett algorithm produces a median error of $-4.69°$ inaccuracy, with estimation errors ranging from $-0.29°$ to $-30.73°$. ESPRIT has a range of error from $-8.56°$ to $16.77°$, with a median error of $-2.93°$. MUSIC ranging from $3.19°$ to $-7.51°$. R-MUSIC performed the best, with the degree of inaccuracy ranging from $3.54°$ to $-5.88°$, with a median of $-1.63°$ offering the best performance. Finally, MVDR estimation errors ranged from $4.19°$ to $-16.34°$.

Further evaluation of the estimator's angular spectrum was conducted to elucidate the impact of the environment on each estimator, as shown in Fig. 3b. For the azimuth angle of $-9.45°$, Fig. 3b shows a comparison of the performance of the five AoA estimation algorithms. The spectral plots for Bartlett, MVDR, and MUSIC are represented by line curves, while the dots represent the estimates for ESPRIT and R-MUSIC. This plot gives an overview of how well each algorithm is able to estimate the AoA values for the incoming signals.

After evaluating multiple AoA estimation algorithms, we chose the Bartlett algorithm for further experimentation. The Bartlett algorithm effectively incorporates a spectrum graph and exhibits higher sensitivity to environmental factors and combines spatial responses to estimate signal angles, providing valuable insights. The spatial response determines signal direction. This information helps detect multi-path or false peaks that can affect angle estimation accuracy.

B. Sample Time

To accurately estimate AoA for mobile drones, we must consider the drone's mobility and physical factors, requiring a significant number of samples to capture channel coherence time. In this study, we determine the necessary number of snapshots for estimating AoA in a time-varying channel by examining the impact of channel coherence time and sampling rate on accuracy. Our findings improve the localization system's overall performance and ensure reliable drone tracking.

Setup: We varied sample sizes from 5 to 5,120 to test the impact on AoA estimation accuracy, using one row of eight antennas in the massive MIMO base station.

Results and Findings: The experiment involved analyzing the data from five different locations, with the estimation results being represented by the error of each location relative to its ground truth. The results of the AoA estimation are plotted against the number of samples in Fig. 4a. The x-axis scale varies exponentially. The results reveal that a higher number of samples result in a smaller deviation of error around the zero mean. In particular, we observed that the line of sight path had the highest estimated peak, which resulted in a more significant number of samples providing the best performance. The shortest time while having the highest accuracy of the estimate was every 64 milliseconds or 320 samples. Thus, a sampling rate of 320 samples or 64 milliseconds will serve as the baseline for monitoring a drone traveling at a maximum speed of 20 m/s.

We observed a degradation in accuracy of $\pm 17°$ after 320 samples, as demonstrated in Fig. 4a. We conducted further investigations into the range of errors, as depicted in Fig. 4b and 4c, for the location of 32.47 degrees when using the Bartlett algorithm. A comparison between Fig. 4b and 4c reveals that the line of sight signal peaked with the greatest response in both cases, while the multi-path signal grew stronger as the number of samples decreased, leading to a conflict in the signals. Additionally, the beamwidth increased and more multi-path was observed in Fig. 4c due to the reduced number of samples. Notably, Fig. 4d illustrates a significant variation from the multi-path at higher sample rates, wherein we observed the multi-path expanding and overlapping to become the primary beam. We further verified the results over multiple instances, which displayed comparable findings.

Our analysis showed that the 320-sample threshold represents the minimum data requirement before observing an increase in estimation max/min range. Such a threshold can vary depending on the channel coherence time and the number of paths. Thus, undersampling results in the detection of the
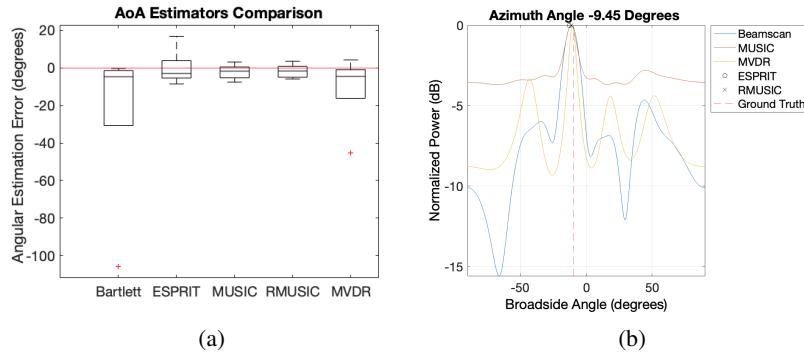
Fig. 3: (a) Comparison of AoA methods using all measured locations. (b) Spatial spectral plots for a specific location.
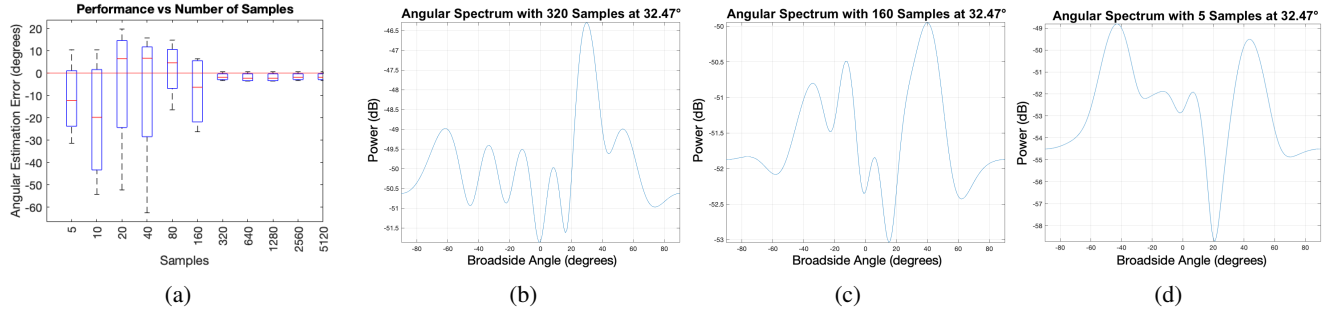

Fig. 4: (a) AoA Bartlett estimation vs the number of samples. (b) 320 samples spectrum graph of the AoA estimation. (c) 160 samples spectrum graph of the AoA estimation. (d) 5 samples spectrum graph of the AoA estimation.

multi-path with higher normalized power, thereby adversely affecting the accuracy of the AoA estimate. While further research is needed to understand the underlying mechanisms and generalize the results to other scenarios, our findings suggest that the 320-sample (corresponding to a sample every 64 milliseconds with a maximum speed of 20 m/s) threshold is a reliable estimate of the minimum data requirement for accurate AoA estimation in our experimental setup.

C. Azimuth Antenna ULA Sizing

The number of antennas and antenna spacing are parameters that influence beamwidth. While antenna spacing is often pre-defined with the minimum length being half of the wavelength in many deployments, massive MIMO systems employ different antenna configurations. As the number of array elements increases, the accuracy of direction-finding algorithms is known to improve. In the azimuth plane, the Argos V3 platform [11] supports up to eight antennas, while the massive MIMO base station boasts five rows, enabling a more comprehensive evaluation. In this section, we investigate the effects of varying the number of antennas on AoA estimation and assess the performance of antenna configurations.

Setup: This study evaluated the performance of two to eight antenna contiguous combinations for estimating AoA of a signal transmitted by a UAV using a 4×8 array. We examine how the vertical array size affects the elevation AoA estimate resolution and present results for different sizes and

combinations. The analysis was performed for each pair and row from the base station.

Results and Findings: Our analysis of various linear array antenna sizes for massive MIMO to drone communications indicates that increasing the number of antennas improves estimation accuracy. Fig. 5 depicts how the number of antennas impacts the estimation accuracy. The estimate ranges from $-6.24°$ to $2.15°$ when eight antennas are used, with an improvement in median accuracy of $3.91°$ for array sizes of two to eight. The graph suggests that accuracy improves as the number of antennas increases.
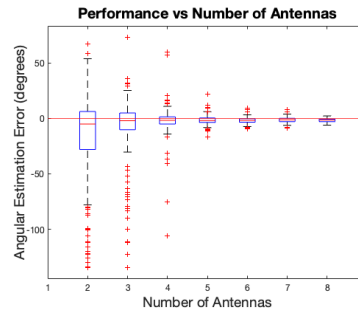

Fig. 5: AoA estimation vs Number of antennas.

The results presented in Fig. 6 show the impact of numbers of antennas on the beam pattern at a single location corresponding to $-9.64°$, where also it can observed that the estimation accuracy improved with an increase in the number

of antennas. Among the different antenna configurations, the eight antennas produced the best result, with an error of only $0.74°$ from the ground truth. On the other hand, the configuration with only two antennas showed a significant deviation of $11.76°$ from the ground truth.
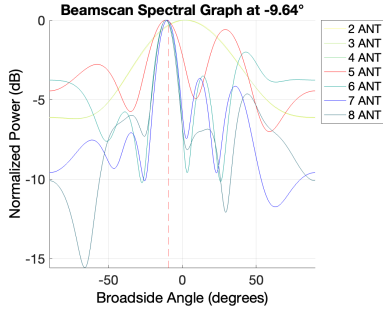

Fig. 6: Bartlett performance for varying number of antennas.

We also found that the effects of multipath on AoA estimates for hovering drones become more pronounced as the number of antennas decreases. Fig. 6 shows the impact of decreasing the number of antennas on the effects of multipath, specifically how the stadium environment affects the AoA estimation. The lower part of the Rice football stadium has cement bleachers on the left side and reflective metallic bleachers on the right side. These reflections appear in the signal when the drone is lifted to an altitude and transmits an omnidirectional signal, resulting in a multi-path influenced by the stadium objects. As shown in Fig 6, the graphs demonstrate the effect of decreasing the number of antennas and the influence of reflective objects on the accuracy of AoA estimation. The results reveal that reducing the number of antennas amplifies the impact of multipath, leading to less accurate AoA estimation.

D. Multi 1-D Azimuth Estimation

AoA estimation relies on the computation of phase shifts of the received antennas, which differ for different rows in a massive MIMO system. This phase estimate improves as the number of antennas increases in a ULA design. While a ULA can be effective for certain applications, the increasing use of multi-ULA and MIMO systems has led to Uniform Rectangular Array (URA) systems outperforming ULAs [10]. The received signal phases differ across the five rows of the URA array, with a vertical spacing 66.68 mm (1.25 wavelengths) between the rows. In addition to antenna spacing, the mobility of the drones and variable channel conditions affect the AoA calculation. In this section, we present the results of evaluating each antenna row set for AoA estimation and averaging the outcomes.

Setup: We used the full 5×8 massive MIMO URA with varying inter-row phase differences.

Results and Findings: Fig. 7 shows the performance of averaging the results from each row estimation. The x-axis shows the number of rows used for estimation while the y-axis shows the estimation error. To combine the results from

different row estimations, we use averaging. Each row is individually used for AoA estimation using its corresponding antennas, and the estimated angles from each row are then averaged to obtain a final estimation.

The range of the estimator decreases as the number of rows increases, with the minimum number of rows, (one row of eight-antennas) having a range of $-6°$ to $2°$. The median estimation error improves by $0.58°$ from one to five rows. The maximum number of rows used is five, providing a $3°$ range compared to an $8°$ range with one row due to variable combinations in the AoA calculation. The design allows for independent observations due to the significant separation of 6.66 cm between each row, which results in varying spatial sums with multi-paths.
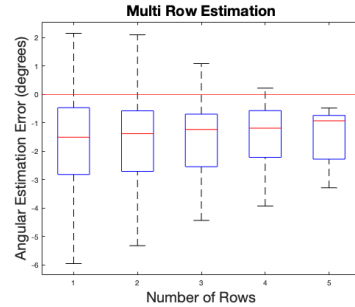

Fig. 7: AoA result for azimuth multi row estimation.

Thus, we observed that each row of the massive MIMO test bed has rich multipath components that result in varying spatial sums, which can lead to high deviation in the AoA estimation. However, despite these fluctuations, we observed a boost in the accuracy of AoA estimation when utilizing massive MIMO estimates obtained from each row by averaging the spectra to obtain a more robust estimate of the AoA. By using multiple rows for their spatial components, we can decrease the range of the estimations and achieve better accuracy overall. Combining the spatial components from multiple rows provides a more complete picture of the signal, allowing for a more accurate estimation of the AoA.

E. Multi 1-D vs 2-D AoA methodology

With the expanding use of massive MIMO, joint azimuth and elevation estimation methods are becoming more important. As a result, attention has increased on the application of 2-D AoA estimation, which involves a search for a two-dimensional spectrum of the angles of arrival of incoming signals [12]. In our experiment, we evaluate the performance of 2-D estimation in comparison to multi-row and column estimation as discussed in Section IV-D for elevation estimation.

Setup: We used a similar algorithm as in Section IV-D to estimate elevation angles from the same set of antennas. The aim was to compare 2-D estimation to multi-row and multi-column estimation and explore the best way to utilize 2-D AoA from the five locations [13].

Results and Findings: Fig. 8a depicts the AoA estimation accuracy for two different approaches: the 2-D Bartlett spatial
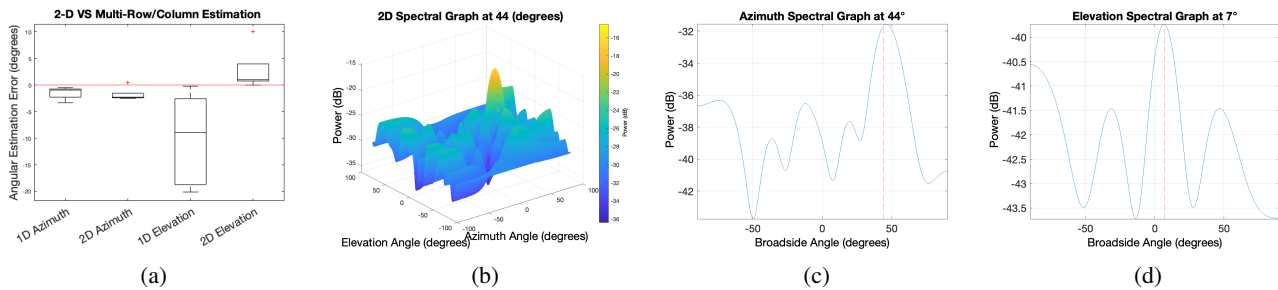
Fig. 8: (a) Comparison between 2-D AoA estimation and multi 1-D AoA estimation. (b) Full 2-D estimation spectrum plot. (c) Azimuth 1-D spectrum plot. (d) Elevation 1-D spectrum plot.

spectrum estimate and the multi-row/azimuth 1-D spectrum and multi-column/elevation 1-D spectrum estimation. The 2-D Bartlett spatial spectrum estimate improves accuracy by aggregating all antennas in the array to locate the spectrum peak. In contrast, the 1-D method finds a peak from each row or column individually, relying on a limited subset of array elements for estimation. By aggregating all antennas, the 2-D Bartlett approach captures subtle differences in angles more effectively, leading to improved accuracy.

The spectrum graphs in Fig. 8b, 8c, and 8d provide a visual comparison of the estimators' peaks between the 2-D and multi-row and column approaches. The 2-D Bartlett estimator exhibits a narrower bandwidth on average, resulting in higher precision and accuracy for azimuth and elevation angles.

Based on our study, the 2-D Bartlett spatial spectrum estimator shows promise for joint azimuth and elevation estimation in massive MIMO systems. It aggregates all antennas to locate the spectrum peak, capturing subtle angle differences missed by the 1-D method. This improves elevation estimation accuracy significantly. The narrower bandwidth of the 2-D estimator also enhances precision and accuracy for both azimuth and elevation angles. These findings are important for designing and optimizing high-precision spatial angle estimation in massive MIMO systems.

V. CONCLUSION

We analyzed five AoA estimation methods for massive MIMO in drone networks and found that R-MUSIC had the best accuracy. However, we used the Bartlett algorithm for further experiments due to its sensitivity to the environment. We discovered that undersampling reduces accuracy, and more than 320 samples reduce multi-path effects and lower estimation errors. Increasing the number of azimuth antennas enhances estimation results, with six to eight antennas offering acceptable consistency. We also observed an improvement in AoA estimation by utilizing massive MIMO and averaging row estimation results. Additionally, 2-D Bartlett spatial spectrum estimation shows potential for joint azimuth and elevation estimation. Our study highlights the importance of accurate AoA estimation in optimizing performance and provides insights for developing more efficient massive MIMO systems for drone networks.

REFERENCES

[1] J. Güldenring, P. Gorczak, F. Eckermann, M. Patchou, J. Tiemann, F. Kurtz, and C. Wietfeld, "Reliable Long-Range Multi-Link Communication for Unmanned Search and Rescue Aircraft Systems in Beyond Visual Line of Sight Operation," *Drones*, vol. 4, no. 2, 2020. [Online]. Available: https://www.mdpi.com/2504-446X/4/2/16

[2] M. Mozaffari, W. Saad, M. Bennis, Y.-H. Nam, and M. Debbah, "A Tutorial on UAVs for Wireless Networks: Applications, Challenges, and Open Problems," *IEEE Commun. Surv. & Tut.*, vol. 21, no. 3, pp. 2334–2360, 2019.

[3] M. A. Sayeed, R. Kumar, V. Sharma, and M. A. Sayeed, "Efficient Deployment with Throughput Maximization for UAVs Communication Networks," *Sensors*, vol. 20, no. 22, 2020. [Online]. Available: https://www.mdpi.com/1424-8220/20/22/6680

[4] A. Sayed, A. Tarighat, and N. Khajehnouri, "Network-based wireless location: challenges faced in developing techniques for accurate wireless location information," *IEEE Sig. Process. Mag.*, vol. 22, pp. 24 – 40, 08 2005.

[5] G. Geraci, A. Garcia-Rodriguez, L. Galati Giordano, D. López-Pérez, and E. Björnson, "Understanding UAV Cellular Communications: From Existing Networks to Massive MIMO," *IEEE Access*, vol. 6, pp. 67 853–67 865, 2018.

[6] J. Xiong and K. Jamieson, "ArrayTrack: A Fine-Grained Indoor Location System," in *Proc. of the 10th USENIX Conf. on Networked Sys. Design Implementation*. USA: USENIX Association, 2013, p. 71–84.

[7] K. Raghu and N. P. Kumari, "Performance Evaluation and Analysis of Direction of Arrival Estimation Algorithms using ULA," in *2018 Int. Conf. Elect., Electron., Commun., Comp., and Optim. Tech. (ICEEC-COT)*, 2018, pp. 1467–1473.

[8] T. Tuncer and B. Friedlander, *Classical and Modern Direction-of-Arrival Estimation*. Elsevier Science, 2009. [Online]. Available: https://books.google.com/books?id=1aQbxKJI2CsC

[9] R. Petrolo, Y. Lin, and E. Knightly, "ASTRO: Autonomous, Sensing, and Tetherless NetwoRked DrOnes," in *Proc. 4th ACM Workshop Micro Aerial Vehicle Networks, Systems, and Appl.*, ser. DroNet'18. New York, NY, USA: Association for Computing Machinery, 2018, p. 1–6. [Online]. Available: https://doi.org/10.1145/3213526.3213527

[10] R. Doost-Mohammady, O. Bejarano, L. Zhong, J. R. Cavallaro, E. Knightly, Z. M. Mao, W. W. Li, X. Chen, and A. Sabharwal, "RENEW: Programmable and Observable Massive MIMO Networks," in *2018 52nd Asilomar Conf. Sig., Sys., Comput.*, 2018, pp. 1654–1658.

[11] C. W. Shepard, R. Doost-Mohammady, R. E. Guerra, and L. Zhong, "Demo: ArgosV3: An Efficient Many-Antenna Platform," in *Proc. 23rd Annu. Int. Conf. Mobile Comput. Netw.*, ser. MobiCom '17. New York, NY, USA: Association for Computing Machinery, 2017, p. 501–503. [Online]. Available: https://doi.org/10.1145/3117811.3119863

[12] H. Miao, M. Juntti, and K. Yu, "2-D Unitary ESPRIT Based Joint AoA and AoD Estimation for MIMO System," in *2006 IEEE 17th Int. Symp. Pers., Indoor Mobile Radio Commun.*, 2006, pp. 1–5.

[13] Y. Zhao, Y. Zhang, and J. Song, "Active Phased Array Radar-based 2D Beamspace MUSIC Channel Estimation for an Integrated Radar and Communication System," in *2019 IEEE 9th Int. Conf. Electron. Info. Emergency Commun. (ICEIEC)*, 2019, pp. 56–60.